Clays and Clay Minerals, Vol. 58, No. 1, 52–61, 2010.

THE COMBINED INELASTIC NEUTRON SCATTERING (INS) AND SOLID-STATE DFT STUDY OF HYDROGEN-ATOMS DYNAMICS IN KAOLINITE-DIMETHYLSULFOXIDE INTERCALATE

L'UBOMÍR SMRČOK[1,*], DANIEL TUNEGA[1,2], ANIBAL JAVIER RAMIREZ-CUESTA[3], ALEXANDER IVANOV[4], AND JANA VALÚCHOVÁ[1]

[1] Institute of Inorganic Chemistry, Slovak Academy of Sciences, Dúbravská cesta 9, SK-845 36 Bratislava, Slovak Republic
[2] Institute of Soil Research, University of Natural Resources and Applied Life Sciences, Peter Jordan Strasse 82, A-1190 Vienna, Austria
[3] ISIS Facility, Rutherford Appleton Laboratory, Chilton, Didcot, Oxon OX11 0QX, United Kingdom
[4] Institute Laue-Langevin, 6 rue Jules Horowitz, 38042, Grenoble, Cedex 9, France

Abstract—Vibrational spectra of two kaolinite-dimethylsulfoxide intercalates, obtained using inelastic neutron scattering (INS), were analyzed with a view to understanding the dynamics of the hydrogen atoms in the structure. The main focus was on the spectral region 0−1700 cm^{-1}, which is difficult to analyze using optical spectroscopy. The experimental vibrational spectra of kaolinite:dimethylsulfoxide and kaolinite:d6-dimethylsulfoxide collected using two different spectrometers were interpreted by means of the solid-state DFT calculations. Calculated spectra were obtained by both normal-mode analysis and molecular dynamics going beyond the harmonic approximation. The Al−O−H bending modes were found to be spread over the large interval 100−1200 cm^{-1}, with the dominant contributions located between 800 and 1200 cm^{-1}. The shape of the individual hydrogen spectrum depends on whether or not the respective hydrogen atom is involved in an O−H···O hydrogen bond and on its strength. The modes corresponding to the in-plane movements of the inner-surface hydrogen atoms are well defined and always appear at the top of the intervals of energy transfer. In contrast, the modes generated by the out-of-plane movements of the hydrogen atoms are spread over large energy intervals extending down to the region of external (lattice) modes. The C−H modes are concentrated mainly in the three regions 1200−1450 cm^{-1}, 800−1100 cm^{-1}, and 0−400 cm^{-1}. While the first two regions are typical of the various deformational modes of methyl groups, the low-energy region is populated by the modes corresponding to the movements of the whole dimethylsulfoxide molecule.

Key Words—DFT, DMSO, Hydrogen Bonds, INS, Kaolinite, Vibrational Spectra.

INTRODUCTION

The present study is an extension of previous computational work on hydrogen bonding in the kaolinite:dimethylsulfoxide (K:DMSO) and kaolinite:dimethylselenoxide (K:DMSeO) intercalates (Scholtzová and Smrčok, 2009; hereafter SCS). Accurate structural data for both intercalates were obtained in the 2009 work and the geometries of all the relevant O−H···O and C−H···O hydrogen bonds were analyzed in detail and theoretically calculated vibrational density of states between 0−4000 cm^{-1} were provided along with the detailed assignments of the individual vibrational modes. The intercalated molecules of DMSO (DMSeO) were found to be fixed in the interlayer space mainly by the three O−H···O hydrogen bonds of different strengths, while the substantially weaker C−H···O and O−H···S (O−H···Se) contacts play a supporting role only (Figure 1). Changes in the calculated vibrational spectra resulting from the formation of new hydrogen bonds involving intercalated molecules were also discussed.

Whereas the O−H stretching modes are of primary interest with regard to the routine characterization of hydrogen bonds in kaolinite intercalates by optical spectroscopies (IR, Raman), Al−O−H and/or *X*−C−H deformation modes are not of such interest. The main reason is that in IR/Raman spectra these modes are obscured by the vibrational modes originating from the stretching movements of the bonds linking the atoms forming either the 1:1 layer or the intercalating organic molecules (Figure 2). In comparison to the stretching modes, these modes are distributed over a larger interval of energies, making their analysis even more complicated.

Inelastic neutron scattering (INS) spectroscopy may provide a solution to this problem because in an INS spectrum of a hydrogenous system the scattered intensity is dominated by the contributions from the hydrogen atoms only. The incoherent scattering cross-section of H (80 barns) is normally much greater than the incoherent scattering cross-sections of other elements present in the compound and so the contribution of the other elements can be ignored without affecting the accuracy. The

* E-mail address of corresponding author:
lubomir.smrcok@savba.sk
DOI: 10.1346/CCMN.2010.0580105

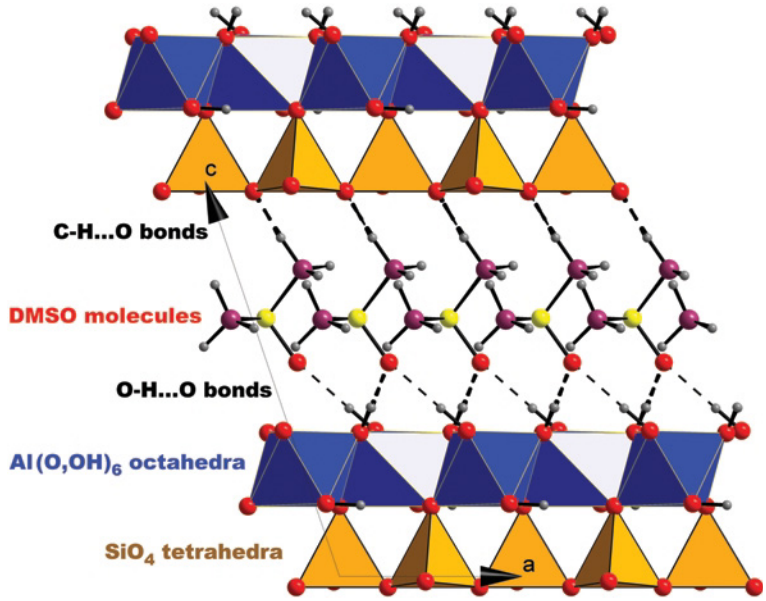

Figure 1. Schematic presentation of the structure of kaolinite intercalated by DMSO viewed along the *b* axis. O–H···O and C–H···O hydrogen bonds are depicted by dashed lines. Figures 1 and 3 were prepared by the *Diamond* program (Brandenburg, 2006).

readability of a spectrum can be further improved by selective deuteration of the hydrogen sites that are of less interest or importance (Mitchell *et al.*, 2005), thereby reducing the contribution of the unwanted hydrogen sites to the spectrum.

Although the contributions by all atoms other than H are negligible and the lack of any selection rules typical of optical spectroscopy make INS spectra more readable, their interpretation is not always straightforward. Fortunately, the power of neutron scattering as a probe

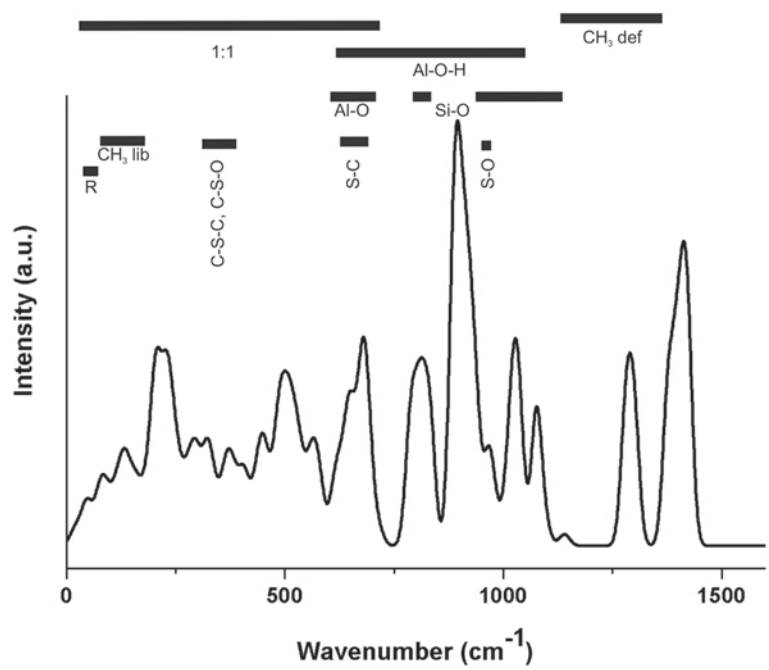

Figure 2. Calculated total vibrational density of states (VDOS) for the K:DMSO interlacate as obtained in the Scholtzová and Smrčok (2009) study. The regions with the most important vibrational modes are indicated by the black lines along the top of the figure. 'R' indicates a region of rocking movement of the molecules.

of hydrogen-atom dynamics can be further enhanced by combining it with the predictive capabilities of theoretical methods, especially of solid-state density functional theory (DFT) calculations based on the known crystal structures of the respective compounds. By comparing experimental INS spectra with theoretically predicted spectra and taking into consideration the relevant structural details, one can reliably interpret the individual vibrational modes involving the hydrogen atoms present in the structure. Although the number of studies of combined INS/theoretical calculations has been growing steadily (see *e.g.* the references in Sládkovičová *et al*., 2008), to the present authors' knowledge, no such combined study of an intercalated layer silicate has been reported so far. In fact, INS studies of layer silicates are quite rare (Wada and Kamitakahara, 1991; Fan *et al*., 1992; Johnston *et al.*, 2000; Chaplot, 2002), although some powerful spectrometers are available at several large facilities around the world.

The aim of the present study was to interpret the INS spectrum of the K:DMSO intercalate within the low- and middle-energy ranges (0−1700 cm^{-1}) by means of theoretical calculations using the solid-state DFT method. Partial vibrational density of states (PVDOS), the main tool used in the study, of hydrogen atoms were obtained within the harmonic approximation (normal mode analysis, NMA) as well as by the alternative approach, molecular dynamics calculations going beyond the harmonic approximation. In spite of the fact that the intensities of such calculated spectra are not directly comparable to those obtained by INS spectroscopy, they provide an excellent insight into the nature of the individual vibrational processes. To improve the separation of the individual modes, the spectra were measured for the kaolinite samples intercalated with hydrogenated and deuterated DMSO.

EXPERIMENTAL AND CALCULATION

Well ordered kaolinite from Gold Field (Tanzania) was used as the raw material. The chemical composition of the original sample is (wt.%): 46.81 SiO_2, 36.72 Al_2O_3, 1.26 Fe_2O_3, 0.08 CaO, 0.06 MgO, 0.08 Na_2O, 0.89 TiO_2, and 0.28 K_2O.

Dimethyl sulfoxide (DMSO, ACS spectrophotometric grade, 99.9%, Sigma-Aldrich) and deuterated dimethyl-d6 sulfoxide (DMSO-d6, 99.9% D, Chemodex.com-customized molecules, Switzerland) were used as received. To prepare the K:DMSO sample, ~1 g of kaolinite was mixed with 5 mL of DMSO and stirred in the dark under a reflux at 85ºC for 72 h. The excess DMSO was removed by subsequent drying at 75ºC. To obtain a deuterated sample (d6-K:DMSO), 5 g of kaolinite was mixed with 40 mL of DMSO-d6 and treated as above. The status of intercalation and of the drying processes was checked by high-resolution powder X-ray diffraction.

The INS spectrum of the K:DMSO intercalate was measured using the TOSCA spectrometer at the ISIS Facility at the Rutherford Appleton Laboratory (Mitchell *et al.*, 2005). The spectra were collected for a total current of 500 μAmp.h at a temperature of 25 K. TOSCA is a high-resolution, broad range, inverse-geometry spectrometer which is well suited to the spectroscopy of hydrogenous materials. The energy transfer is from 16 to 4000 cm^{-1}, with an instrumental resolution of $\Delta E/E$ <1.4%.

The spectrum of d6-K:DMSO was recorded using the IN1-BeF spectrometer installed at the hot source of the high-flux reactor at the Institute Laue-Langevin, Grenoble (see http://www.ill.eu/tas for details). Two monochromators, Cu220 and Cu331, were used to cover the incident neutron energy range from 40 to 520 meV (320−4160 cm^{-1}). A Soller slit collimator reduced the monochromatic beam divergence down to 20' resulting in an energy resolution of 3−4% for Cu331 and 4−6% for Cu220. The powder sample was placed in a 2-mm thick, flat aluminum container sealed with an indium metal joint and maintained at 11 K using a helium closed-cycle refrigerator.

Details of the calculations of the normal modes and of the partial vibrational densities of states under harmonic approximation were documented in the SCS study, and only the essentials of the calculations using VASP code (Kresse and Hafner, 1993; Kresse and Hafner, 1994; Kresse and Furthműller, 1996) are repeated here.

The energy cutoff controlling the accuracy of the calculation was set to 500 eV and the structure was optimized by a conjugated gradient method in four *k* points. Normal modes of vibrations were calculated within the computational cells from the normal mode analysis accomplished in the frames of the harmonic approximation. In the normal mode calculation, the total energy converged to 10^{-7} eV and residual forces on the atoms were <0.005 eV/Å. To interpret the INS spectra the 'H' model, assuming half occupation of the expected positions of the organic molecules in the structure of the intercalate, was used (Figure 3A). The full geometry of this model can be found in the SCS paper.

The normal mode calculations taken from the SCS study were complemented by the molecular dynamics calculations (MD) carried out using the same code. The energy cutoff was reduced to 400 eV, the number of *k* points was two, and the required convergence in total energy was 10^{-4} eV. The finite temperature calculations were performed on a canonical ensemble with a Nosé thermostat procedure (Nosé, 1984) at the simulation temperature of 300 K. The Verlet velocity algorithm (Ferrario and Ryckaert, 1985) with a time step of 1 fs was chosen and a total of 65 ps of MD was calculated. The results of the MD calculations were interpreted in frequency space by calculating the Fourier transform of the individual velocity autocorrelation functions and

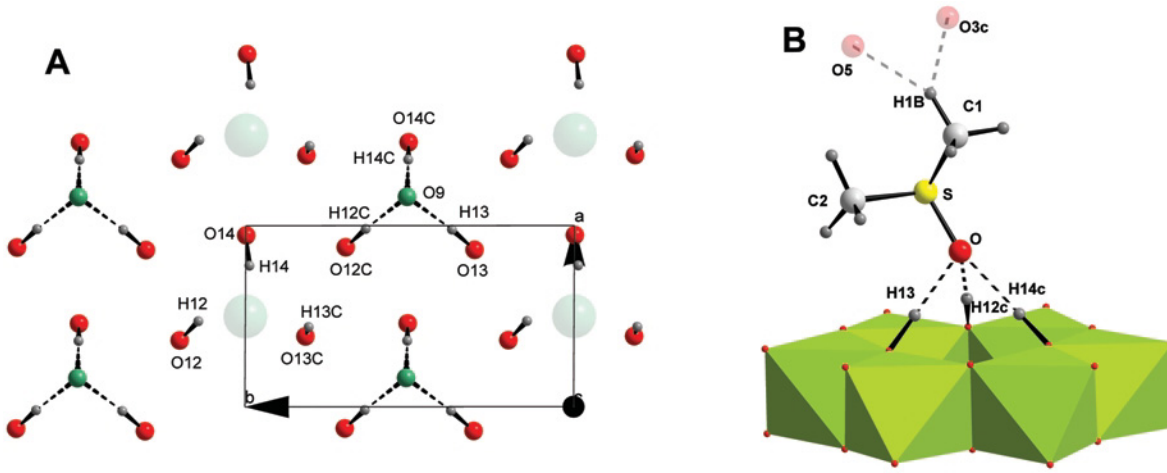

Figure 3. (A) Orientation of the inner-surface O–H bonds in the computational model shown along the *c* axis. Large gray balls indicate missing organic molecules. (B) Hydrogen bonds formed by the three inner-OH groups and DMSO. Two possible C–H···O contacts to the adjacent 1:1 layer are depicted in a pale color.

presented in the form of power spectra (PS) (see *e.g.* Kirkpatrick *et al*., 2005). Vibrational densities of states in the harmonic approximation were calculated using the *AClimax* code (Ramirez-Cuesta, 2004).

RESULTS AND DISCUSSION

General considerations

Taking into consideration that very mixed modes are characteristic of the INS spectrum of the K:DMSO intercalate, the vast majority of the peaks cannot be easily associated with a single fundamental energy. From a graphical comparison (Figure 4), the calculated C–H and O–H vibrational densities of states obviously overlap almost perfectly, the exceptions being two peaks localized in the C–H spectrum at ~1415 and 1293 cm^{-1} and the broad band in the O–H spectrum centered around ~500 cm^{-1}. Perfect overlap of the C–H and O–H modes is also noted from comparison of the two experimental spectra. Note that because access to the low-energy region with the IN1-BeF spectrometer is practically limited to the minimum of ~320 cm^{-1}, not all the calculated low-energy O–H modes could be seen to be measured. The sharp, well structured peaks in the K:DMSO spectrum are concentrated in the <500 cm^{-1} region, which mostly contains the contribution from the C–H modes. However, the low-energy part of the spectrum could contain the internal modes 'contaminated' by the rotational and translational motions of the DMSO molecules and hence their formal attribution as internal modes may be somewhat approximate. The d6:K-DMSO spectrum contains few well pronounced features mirroring the movements of both hydrogen-bonded and 'free,' *i.e.* unbound, OH groups. In all the following analyses of the spectra, the authors refer to the collection of the unscaled modes presented in Appendix A of the SCS paper.

C–H modes

Because no significant difference exists in the shapes of the densities of states and the power spectra obtained for the hydrogen atoms of either methyl group, they are neither shown nor analyzed in the following. For the purposes of the proposed analysis, the calculated PVDOS values can be formally divided into four non-overlapping regions (Figure 5). In the first, between 1500 and 1200 cm^{-1}, only two well separated features are recognized. The bands centered closer to 1400 cm^{-1} are formed by a combination of the out-of-plane (*op*) and in-plane (*ip*) deformation modes predicted at 1423,

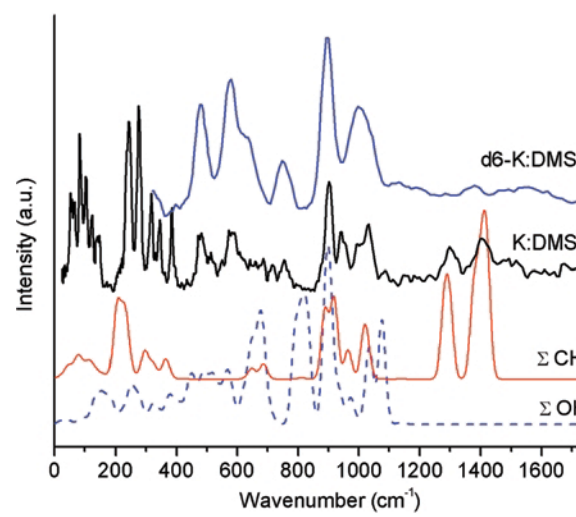

Figure 4. A comparison of the measured d6-K:DMSO and K:DMSO INS spectra and the sums of the partial CH and OH vibrational densities of states. The spectra are offset for the purposes of clarity. Note that because all the individual spectra throughout the paper are scaled to their respective maxima, the scales on the vertical axes are arbitrary.

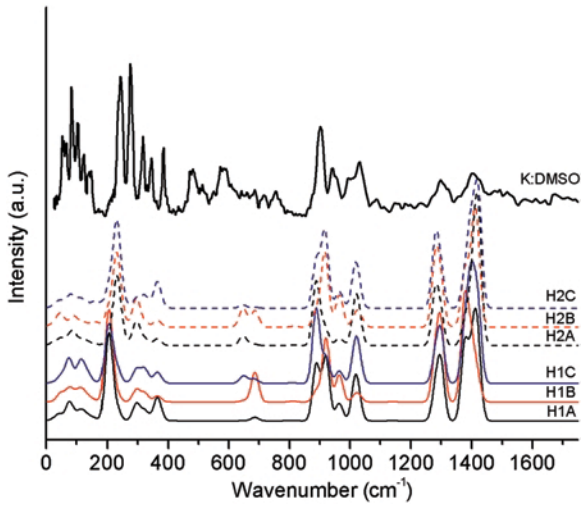

Figure 5. Calculated partial vibrational density of states for the respective hydrogen atoms of the methyl groups of the DMSO molecule are presented in two bands with the measured INS spectrum on the top. The atoms labeled H1*x* belong to the methyl group situated closer to the adjacent 1:1 layer (*cf.* Figure 3). The spectra are offset for the purposes of clarity.

1412, 1398, and 1377 cm^{-1}. The two higher-energy modes reflect the *op* movements of the hydrogen atoms bonded to the C2 atom (Figure 3B) and the *ip* modes of the hydrogen atoms along the C1 atom. In contrast, two lower-energy modes appear due to both *op* and *ip* movements of the H-atoms of both methyl groups. The next band at ~1280 cm^{-1} is formed by two almost pure *op* modes (1300, 1282 cm^{-1}) of both methyl groups. All the calculated CH modes appearing between 1500 and 1200 cm^{-1} have their counterparts in the two broad peaks centered in the experimental INS spectrum at ~1400 and 1290 cm^{-1}. Such modes have also been documented in the Raman study of a K:DMSO intercalate by Martens *et al*. (2002), who assigned two maxima at 1430 and 1411 cm^{-1} to the *ip* bending mode of a methyl group. In the IR spectrum of a K:DMSO intercalate, Olejnik *et al.* (1968) identified the four bands (1431, 1412, 1397, and 1313 cm^{-1}) as both asymmetric and symmetric methyl-group deformations. In pure DMSO (vapor phase and liquid), the six bands detected between 1455 and 1304 cm^{-1} were assigned by Horrocks and Cotton (1961) to the rather general category 'degenerate methyl group deformation.'

The calculated band structure of the second region (1100–640 cm^{-1}) contains two clusters of the peaks which differ significantly in their intensities (Figure 5). While the first cluster contains easily recognizable maxima centered at ~1020, 960, and 900 cm^{-1}, the second consists of several weak contributions with the central peak at ~690 cm^{-1}. The peaks at the higher energies (1025, 1016, and 963 cm^{-1}) belong to the *op* deformation modes of the methyl groups coupled with the C–S–C bending and S=O stretching movements. Inspection of the SCS results reveals that the contributions to the lower-energy edge of the first cluster are from the *op* modes of the hydrogen atoms of the methyl groups bound to the C1 (922 cm^{-1}) or C2 (918 cm^{-1}) atom; modes reflecting a deformation movement of both methyl groups (889 cm^{-1}) also appear. All these modes contribute to the feature appearing in the INS spectrum between 1110 and 840 cm^{-1}. In the study of pure DMSO, the bands between 1016 and 915 cm^{-1} have been attributed to CH_3 rocking (Horrocks and Cotton, 1961).

The weak peaks gathered in the calculated spectra close to ~690 cm^{-1} are suggested to be due to the symmetric and antisymmetric S–C stretching modes causing a small *op* deformation of the two methyl groups. However, because of their overlap with some calculated O–H modes (Figure 4), they cannot be recognized unambiguously in the experimental spectrum. In previous studies, the peaks observed at 689 and 672 cm^{-1} (Horrocks and Cotton, 1961) or at 672 and 705 cm^{-1} in the Raman study of DMSO (Durig *et al*., 1970) are interpreted as symmetric and anti-symmetric C–S stretching modes. The DMSO band at ~522 cm^{-1} obtained by the INS technique (Safford *et al*., 1969) was assigned to the group of modes belonging to CH_3 rocking and symmetric and anti-symmetric C–S stretching. Unfortunately, the overall accuracy of the latter study is rather poor and the respective values cannot be used as a reference.

Any interpretation of two low-energy regions must be done with some caution because of the possible appearance of external ('lattice') modes, which are not completely covered by the predictive calculations. The bands in the third region (400–160 cm^{-1}) are ascribed to the highly mixed modes: C–S–O bending movements inducing some wobbling of the rigid methyl groups (375–279 cm^{-1}) and/or librations of the methyl groups around the S–C bonds (260–162 cm^{-1}). The most pronounced peaks in this region can be assigned to the oscillation of the methyl groups around the S–C2 (231 cm^{-1}) and S–C1 (206 cm^{-1}) bonds. These different energies clearly document the inequality of both $-CH_3$ groups in the structure. The counterparts in the experimental INS spectrum are the sharp transitions appearing at ~384, 344, 316, 272, and 242 cm^{-1} which were poorly documented in the previous studies and, if detected, were attributed to C–S–O and C–S–C bending deformations (Horrocks and Cotton, 1961; Safford *et al*., 1969; Durig *et al*., 1970).

The fourth region in the INS spectrum with the lowest-energy peaks at ~159–133, 121, 103, 82, and 72–25 cm^{-1} reflects various 'rocking' rigid-body movements of the DMSO molecules. In previous experimental studies the bands in this region have been interpreted as unspecified librational and translational movements (147–70 cm^{-1}, Durig *et al*., 1970) or as "lattice modes" (165–32 cm^{-1}, Safford *et al*., 1969).

O–H modes by Normal Mode Analysis

Within the current structural model, the O–H···O hydrogen bonds found in the K:DMSO structure are among those considered to be 'moderately strong' (Steiner, 2002). If taking the O···O separation as a measure of hydrogen-bond strength, the weakest are the bonds involving the H14c atoms and the strength increases for the bonds including the H13 and H12c hydrogen atoms (Figure 3A). Because the computational model assumes 50% intercalation, in the computational cell three inner-surface hydroxyl groups exist (with H12, H14, and H13c hydrogen atoms), which have no partners for the formation of hydrogen bonds and can thus freely reorient within the interlayer space in order to reach an energy minimum. In the SCS study, those atoms were found to produce spectra which are quite different from those of the hydrogen-bonded ones.

The strongest features in the PVDOS values calculated for the inner hydroxyl H11/H11c atoms localized at ~910 cm^{-1} (Figure 6a) reflect in-phase movement of both hydrogen atoms in the plane approximately parallel to the plane defined by the apical oxygen atoms of the SiO_4 tetrahedra. Less intensive peaks predicted at the lower energies (685, 639, 575, and 563 cm^{-1}) result from both in-phase and out-of-phase Al–O–H bending movements in the directions approximately perpendicular to that plane. The peaks at very low energies, visible in the calculated spectrum in the region down to 125 cm^{-1}, appear because of several slow deformations of the complete 1:1 layer resulting in the changes of the position of the H11 and H11c atoms. The position of the main peak (~910 cm^{-1}) agrees well with the position of the intense band in the INS spectrum at ~908 cm^{-1}. Such an in-plane mode has been found at 915 cm^{-1}, for example, in the Raman spectrum of a kaolinite powder (Frost and Kloprogge, 1999) or at 919/921 cm^{-1} in the single-crystal Raman spectrum of dickite (Johnston *et al*., 1998).

Involvement of the three inner-surface hydroxyl hydrogen atoms in the O–H···O hydrogen bonds has significant impact not only on the positions of the dominant modes, but also on the shape of the individual PVDOSs. The predicted patterns of the hydrogen bonded atoms (Figure 6) are clearly less structured and the modes do not span to the low-energy edge. On the contrary, the much greater freedom enjoyed by the non-hydrogen-bonded atoms gives rise to a plethora of weak, low-energy features, representing highly mixed modes. Involvement of the H12c atom in the strongest O–H...O bond in the structure (d(O···O) = 2.739 Å, O–H···O bond angle = 174°) has caused one of its Al–O–H bending modes to appear on the top of the predicted spectra of all the hydroxyl hydrogen atoms in the structure at 1077 cm^{-1} (Figure 6a). Inspection of the list of modes in the SCS study shows that this mode is present due to hydrogen-atom movement in the plane (*ip*) parallel to the plane defined by the oxygen atoms of the inner-surface hydroxyl groups. The other two modes predicted at 806 and 688 cm^{-1} are assigned to the Al–O–H out of (this) plane (*op*) deformation vibrations and correspond to the broad band in the INS spectrum at ~1004 cm^{-1} and to the bands at 754 and 641 cm^{-1}, respectively.

From comparison of the bands' positions in the calculated and measured spectra, the calculations clearly overestimate at least the positions of the main peaks obtained for the strongly hydrogen-bonded H12c atom. A plausible, though unavoidably rather general, explanation is: (1) the sensitivity of the energies of the O–H modes to the geometry of a hydrogen bond; and (2) the

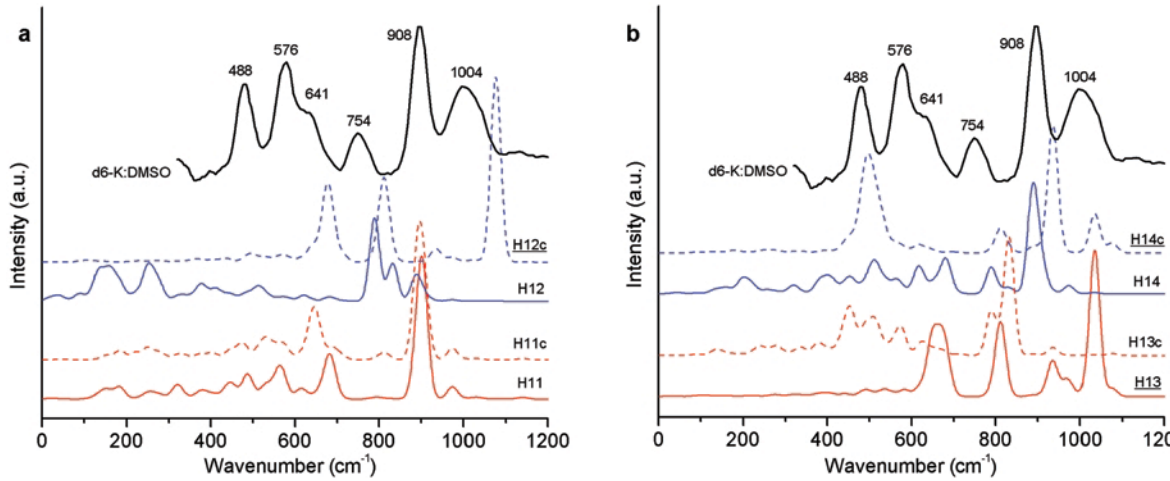

Figure 6. Comparison of the measured d6-K:DMSO INS spectrum and the partial OH vibrational densities of states for H11/H12 (a) and H13/H14 atoms (b) calculated using the harmonic approximation. Underlined atoms are involved in the O–H···O hydrogen bonds. The positions of the peaks in the INS spectrum are estimated as the positions of the local maxima. Each spectrum is offset by a constant for sake of clarity.

tendency of the DFT method to exaggerate the strength of the hydrogen bonds. As a consequence, calculated bending modes might be shifted toward higher energies. Another plausible explanation is neglect of possible anharmonicity in bending vibrations by the standard normal mode analysis procedure used in the harmonic approximation. However, in spite of these differences, the overall agreement between the calculated and observed spectra is relatively good and an unambiguous assignment of the modes can be obtained.

The H12 atom, movement of which is not restricted by a hydrogen bond, behaves rather differently from the bond-constrained H12c. In the case of the H12 atom, the main contributions to the PVDOS come from the three modes (892, 833, and 786 cm^{-1}), which show up due to *ip* Al−O−H deformations (Figure 6a). The modes are reflected by the peaks in the INS spectrum at 908 and 754 cm^{-1}. In contrast to the H12c atoms, the only well defined *op* deformations have their pictures predicted in the region typical for the lattice, rather than for internal modes (260 and 162 cm^{-1}). The weak and heavily overlapping modes framed by these two bunches of well defined modes are strongly coupled with the various 1:1 layer deformations and thus have no well defined pictures in the INS spectrum.

As expected, the situation described above, to a greater or lesser degree, is repeated for the pairs of H13/H13c and H14/H14c hydrogen atoms (Figure 6b). The hydrogen bonds in which the H13 and H14c atoms are involved are weaker compared to the H12c (O···O separations/O−H···O bond angles are 2.784 Å/175º and 2.912 Å/178º, respectively), so that the corresponding blue shifts of the bending modes are comparably smaller. As in the case of H12c, involvement of the respective hydrogen atoms in the hydrogen bonds makes the PVDOSs more readable. The positions of the high-energy *ip* modes for the hydrogen-bonded H13 and H14c atoms appear very close, 1035/936 *vs.* 1035/940 cm^{-1}, but the intensities are reversed (Figure 5b). These *ip* modes are evidently reflected by the INS bands appearing at 1004 and 908 cm^{-1}. The respective Al−O−H *op* modes are reflected by the well recognized bands centered at 808 and 664 (H13), and 813 and 498 cm^{-1} (H14c), respectively. If one accepts that the modes are shifted due to a certain inaccuracy in the calculation, the *op* modes at 813 (H14c) and 808 cm^{-1} (H13) can be assigned to the band in the INS spectrum centered at ~754 cm^{-1}.

Finally, the non-hydrogen bonded H13c and H14 atoms have, compared to the H13 and H14c atoms, well recognized *ip* modes predicted at lower energies, 833/789 and 891/789 cm^{-1}, respectively (Figure 6b). The modes are obviously related to the INS bands centered at ~908 and 754 cm^{-1}. The best resolved Al−O−H *op* modes are predicted at 573/514/455 cm^{-1} (H13c), while for the H14 a whole palette of such deformation modes with similar energy values is possible between 685 and 220 cm^{-1}. At the low-energy edge of the spectrum these modes mix with the modes arising from the various deformations of the 1:1 layer.

O−H modes by molecular dynamics

The general tendency in the calculated power spectra of all inner-surface hydrogen atoms is a multiplet at the higher-energy edge where the NMA predicts *ip* modes and a broad, almost featureless band, spanning, in the cases of the non-hydrogen-bonded atoms, even to the region of the lattice modes (Figure 7a,b). The positions of several peaks, which are recognizable in the individual broad bands, agree within a reasonable limit with the positions of the *op* Al−O−H deformations predicted by the NMA, but in general the broad shape of these bands indicates complicated movements of these hydrogen atoms. To estimate the weight given to each atomic movement by the MD calculation, the ratio of the integrated intensities (integral power) above and below 700 cm^{-1} was used. The breakpoint value was chosen rather arbitrarily, though inspired somewhat by the shape of the PS calculated for the H13c atom, where those two parts are nicely separated.

The main peak of the strongly hydrogen-bonded H12c atom identified as an *ip* mode at 1077 cm^{-1} in the PVDOS (Figure 6a) splits the PS into two overlapped peaks at ~1044 and 1009 cm^{-1} (Figure 7a). The position of this doublet is, in contrast to the PVDOS, in fair agreement with the position of the INS band observed at 1004 cm^{-1}. The peak in the PS at 940 cm^{-1} could be related to the very small peak (*ip*) in PVDOS at 936 cm^{-1}, but the MD emphasizes its role. In other words, while the MD proposes the existence of two kinds of almost equivalent *ip* modes, the NMA strongly infers the existence of a higher-energy one only. The working hypothesis in this case is that the discrepancy may be attributed to anharmonicity unaccounted for by the NMA approach. Whereas the next band in the PS centered at ~790 cm^{-1} appears at approximately the same position as the 806 cm^{-1} *op* mode predicted by the NMA, the broad band peaking at ~600 cm^{-1} evidently has no single counterpart in the PVDOS. The two bands mark the inseparable contributions to the INS bands at 754, to the doublet at 641/576, and to a lesser extent also to the 488 cm^{-1} band. The H12c atom does not contribute much to the low-energy modes as is documented by the ratio of the integral powers above and below the critical energy value (2.6) and also by the fact that the PS disappears at ~500 cm^{-1}.

The positions of the three major bands shaping the multiplet at the higher edge of the PS of the 'free' H12 atom (890, 836, and 790 cm^{-1}) (Figure 7a) are in line with the positions of the three *ip* modes predicted by the NMA analysis (892, 833, and 786 cm^{-1}). The multiplet fits to the region where the INS bands at 908 and 754 cm^{-1} appear. The most striking difference between this PS and the PS of the H12c atom is the shape of the

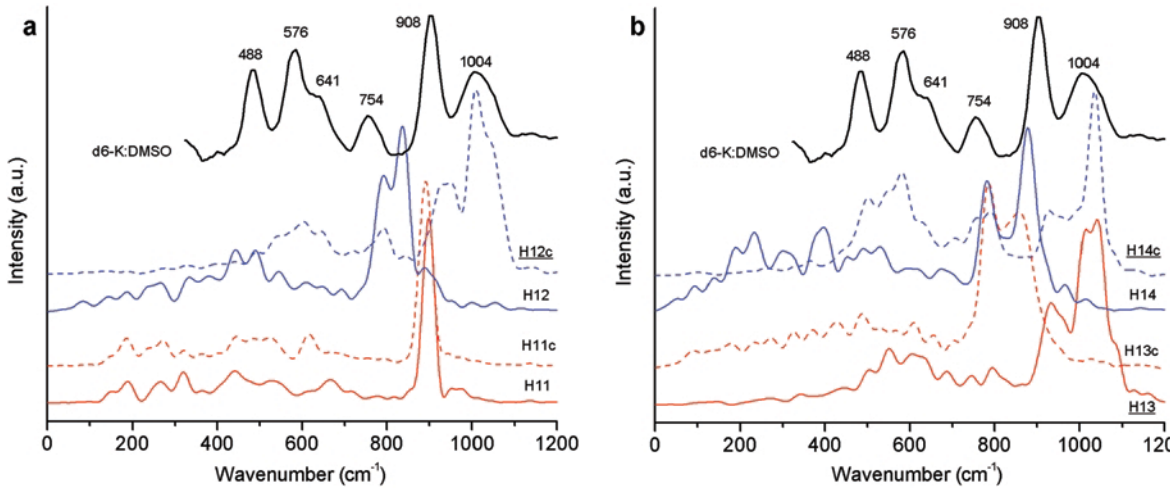

Figure 7. Comparison of the measured d6-K:DMSO INS spectrum and the power spectra obtained by molecular dynamics for H11/H12 (a) and H13/H14 atoms (b). Underlined atoms are involved in the O–H···O hydrogen bonds. The positions of the peaks in the INS spectrum are estimated as the positions of the local maxima. The spectra are offset for the purposes of clarity.

region below 700 cm^{-1}, where the MD predicts a poorly structured continuum peaking at ~500 cm^{-1}, *i.e.* contributing mostly to the INS band at 488 cm^{-1}. On the contrary, in the PVDOS, weight is given to the region below 300 cm^{-1} which, unfortunately, is not documented by the INS experiment carried out at IN1-BeF. Because the ratio of the integral powers is still rather large, 2.5, the energy maximum is still in the *ip* modes.

The maxima identified within the multiplet appearing at the high-energy edge of the PS (Figure 7b) obtained for the hydrogen-bonded H13 atom at ~1040, 1010, and 934 cm^{-1} correspond to the *ip* bands in the PVDOS. However, in contrast to the PVDOS, no such difference was observed in the intensities of the individual bands and the separation between the dominant peaks is smaller. All these modes contribute to the high-energy INS bands at 1004 and 908 cm^{-1}. The *op* modes peaking in the PVDOS at 808 and 664 cm^{-1} have no distinctive counterparts in the PS. The main contributions of the fused modes in the PS go to the lower-energy INS bands 641/576 and 488 cm^{-1}; the contribution to the band at 754 cm^{-1} is moderate.

As for the H13 atom, the positions of the maxima in the PS of H13c (860 and 780 cm^{-1}) also correlate reasonably well with the positions of the *ip* modes predicted by the NMA at 833 and 789 cm^{-1}. The maxima represent the hydrogen movement reflected by the INS band at 908 and 754 cm^{-1}, the contribution to the former is to the band's low-energy edge. In contrast, interpretation of the almost featureless region between 700 and 100 cm^{-1} is difficult. The only reasonable conclusion is that its shape along with the energy ratio dropping from 2.5 for H13 to 1.2 for H13c indicates that, though the nature of their movements is similar, the H13c atom executes remarkably more small-energy movements than H13 (Figure 7b).

A very interesting feature of the PS calculated for the weakly hydrogen-bonded H14c is that its shape resembles that obtained for the strongly bonded H12c rather than that of the less hydrogen-bond-constrained H13 atom. One dominant peak occurs at 1030 cm^{-1} (*cf.* 1035 cm^{-1}, *ip* from the normal mode analysis) with a broad cluster of peaks on the left side with no recognizable maximum. Owing to its broadness it could well contain the *ip* mode predicted at 940 cm^{-1}, but the order of the intensities is reversed compared to the PVDOS. Both of these modes contribute to the INS bands at 1004 and 908 cm^{-1}. The broader peak with the maximum found in the PS at ~780 cm^{-1}, which could correspond to the *op* mode predicted by the NMA at 813 cm^{-1}, correlates with the INS band at 754 cm^{-1}. The broadest cluster in the PS framed by 700 and 400 cm^{-1} contains comparable contributions to the INS doublet 641/576 cm^{-1} as well to the INS band at 488 cm^{-1}. In line with the shape of the PS, the energy ratio is only 1.3 so that this atom spends a considerable time in out-of-plane movements.

The pronounced shift of the spectrum toward the low-energy edge and the energy ratio as low as 0.7 points to the fact that the non-hydrogen bonded H14 is coupled with various low-energy movements of the 1:1 layer. The fact that recognizing any well separated peaks below 700 cm^{-1} (Figure 7b) is not possible seriously hampers any detailed interpretation. Two sharp peaks at 878 and 789 cm^{-1} and reflected by the INS bands at 908 and 754 cm^{-1} can be reconciled with the *ip* modes calculated by NMA at 891 and 789 cm^{-1}, respectively.

The behavior of the modes corresponding to the bending movements of inner-hydroxyl groups OH11/OH11c (Figure 7a) is also intriguing; although they enjoy lesser degrees of freedom for their movement than the hydrogen atoms of the inner-surface hydroxyl

groups, the complexity of the spectra they produce is comparable to the others as some small dispersed peaks can be recognized down to 125 cm^{-1}. The appearance of these low-energy peaks may mirror coupling of the inner-OH bending movement with deformations of the 1:1 layer. The main peak positions found both in the PVDOS and PS spectra are very close, indicating little anharmonicity in the main bending movement of the inner OH groups. The calculated frequency of this mode reveals that this band contributes to the experimental INS peak at 908 cm^{-1}.

CONCLUSIONS

The shape of the individual hydrogen spectrum depends on whether or not the respective hydrogen atom is involved in an O−H···O hydrogen bond and on its strength. The modes corresponding to the in-plane movements of the inner-surface hydrogen atoms are well defined and always appear on top of the intervals of energy transfer. In contrast, the modes generated by the out-of-plane movements of the hydrogen atoms are spread over large energy intervals extending down to the region of external (lattice) modes. The maxima at the high-energy edge of the individual power spectra are in fair agreement with those obtained by the normal mode analysis in the harmonic approximation. The main difference is in the shape of the PS below 700 cm^{-1}. The complexity in the spectra of the bending modes can be assumed to arise from modulation of the changes of the Al−O−H bond angles by a slower-deformation movement of the entire 1:1 layer; the modes are weak and difficult to identify. Neither the predicted involvement of the methyl group around C2 in the weak C−H···O hydrogen bonds nor the long-range interaction of both groups with the adjacent plane of basal oxygen atoms has any noticeable impact on the positions of the modes or on their shapes in the INS spectra.

ACKNOWLEDGMENTS

The SFTC-ISIS Facility and the Institute Laue-Langevin are acknowledged for providing neutron-beam access on the TOSCA and IN1-BeF instruments. The authors acknowledge the financial support of the Slovak Research and Development Agency APVV under contract APVV-51-050505. The work has benefited from the Centers of Excellence program of the Slovak Academy of Sciences (COMCHEM, Contract no. II/1/2007). DT acknowledges the German Research Foundation, priority program SPP 1315, Project GE 1676/1-1.

REFERENCES

Brandenburg, K. (2006) *Diamond*. Version 3.1d. Crystal Impact GbR, Bonn, Germany.

Chaplot, S.L., Choudhury, N., Ghose. S., Rao, M.N., Mittal, R., and Goel, P. (2002) Inelastic neutron scattering and lattice dynamics of minerals. *European Journal of Mineralogy*, **14**, 291−329.

Durig, J.R., Player, C.M. Jr., and Bragin, J. (1970) Low-frequency vibrations of molecular crystals. VII. DMSO and DMSO-d_6. *The Journal of Chemical Physics*, **52**, 4224−4233.

Fan, Y.B., Solin, S.A., Kim, H., Pinnavaia, T.J., and Neumann, D.A.(1992) Elastic and inelastic neutron-scattering study of hydrogenated and deuterated trimethylammonium pillared vermiculite clays. *Journal of Chemical Physics*, **96**, 7064−7071.

Ferrario, M. and Ryckaert, J.P. (1985) Constant pressure-constant temperature molecular dynamics for rigid and partially rigid molecular systems. *Molecular Physics*, **54**, 587−603.

Frost, R.L. and Kloprogge, J.T. (1999) Raman spectroscopy of the low frequency region of kaolinite at 298 and 77 K. *Applied Spectroscopy*, **53**, 1610−1616.

Horrocks, Jr., W.D. and Cotton, F.A. (1961) Infrared and Raman spectra and normal co-ordinate analysis of dimethyl sulfoxide and dimethyl sulfoxide−d_6. *Spectrochimica Acta*, **17**, 134−147.

Johnston, C.T., Helsen, J., Schoonheydt, R.A., Bish, D.L., and Agnew, S.F. (1998) Single-crystal Raman spectroscopic study of dickite. *American Mineralogist*, **83**, 75−84.

Johnston, C.T., Bish, D.L., Eckert, J., and Brown, L.A. (2000) Infrared and inelastic neutron scattering study of the 1.03- and 0.95-nm kaolinite–hydrazine intercalation complexes. *Journal of Physical Chemistry B*, **104**, 8080−8088.

Kresse, G. and Hafner, J. (1993) Ab initio molecular dynamics for open-shell transition metals. *Physical Review B*, **48**, 13115−13118.

Kresse, G. and Hafner, J. (1994) Norm-conserving and ultrasoft pseudopotentials for first-row and transition elements. *Journal of Physics: Condensed Matter*, **6**, 8245−8527.

Kresse, G. and Furthmůller, J. (1996) Efficiency of ab-initio total energy calculations for metals and semiconductors using a plane-wave basis set. *Computational Materials Science*, **6**, 15−50.

Kirkpatrick, R.J., Kalinchev, A.G., Wang, J., Hou, X., and Amonette, J. (2005) Molecular modeling of the vibrational spectra of interlayer and surface species of layered double hydroxides. Pp. 239−285 in: *The Application of Vibrational Spectroscopy to Clay Minerals and Layered Double Hydroxides* (J. Theo Kloprogge, editor). CMS Workshop Lecture Series, **13**, The Clay Minerals Society, Aurora, CO, USA.

Mitchell, P.C.H., Parker, S.F., Ramirez-Cuesta, A.J., and Tomkinson, J. (2005) *Vibrational Spectroscopy with Neutrons*. World Scientific, Singapore.

Martens, W.N., Frost, R.L., Kristof, J., and Horvath, E. (2002) Modification of kaolinite surfaces through intercalation with deuterated dimethylsulfoxide. *Journal of Physical Chemistry B*, **106**, 4162−4171.

Nosé, S.J. (1984) A unified formulation of the constant temperature molecular dynamics methods. *Journal of Chemical Physics*, **81**, 511−519.

Olejnik, S., Aylmore, L.A.G., Posner, A.M., and Quirk, J.P. (1968) Infrared spectra of kaolin mineral-dimethylsulfoxide complexes. *The Journal of Physical Chemistry*, **72**, 241−249.

Ramirez-Cuesta, A.J. (2004) *aCLIMAX* 4.0.1. The new version of the software for analyzing and interpreting INS spectra. *Computer Physics Communications*, **157**, 226−238.

Safford, S.J., Schaffer, P.C., Leung, P.S., Doebbler, G.F., Brady, G.W., and Lyden, E.F.X. (1969) Neutron inelastic scattering and X-ray studies of aqueous solutions of dimethylsulfoxide and dimethylsulphone. *The Journal of Chemical Physics*, **50**, 2140−2159.

Scholtzová, E. and Smrčok, L'. (2009) Hydrogen bonding and vibrational spectra in kaolinite-dimethylsulfoxide and –

dimethylselenoxide intarcalates – a solid state computational study. *Clays and Clay Minerals* **57**, 54–71.

Sládkovičová, M., Smrčok, L'., Mach, P., Tunega, D., and Ramirez-Cuesta, A.J. (2008) Inelastic neutron scattering and DFT study of 1,6-anhydro-β-D-glucopyranose. *Journal of Molecular Structure*, **874**, 108–120.

Steiner, T. (2002) The hydrogen bond in the solid state. *Angewandte Chemie*, *International Edition*, **41**, 48–76.

Wada, N. and Kamitakahara, W.A. (1991) Inelastic neutron-scattering and Raman-scattering studies of muscovite and vermiculite layered silicates. *Physical Review B,* **43** 2391–2397.

(*Received 7 May 2009; revised 31 August 2009; Ms. 315; A.E. T. Kogure*)